TISSUE ENGINEERING: Part C
Volume 28, Number 12, 2022

DOI: 10.1089/ten.tec.2022.0165

termis
Tissue Engineering
& Regenerative Medicine
International Society

Open camera or QR reader and scan code to access this article and other resources online.

***METHODS ARTICLE***

# Three-Dimensional Bio-Printed Autologous Omentum Patch Ameliorates Unilateral Ureteral Obstruction-Induced Renal Fibrosis

Hyunwoo Jo, MS,[1,2] Bo Young Choi, MS,[1] Giup Jang, PhD,[3] Jung Pyo Lee, MD, PhD,[4–6] Ara Cho, MS,[6] Boyun Kim,[1] Jeong Hwan Park, MD, PhD,[7,8] Jeonghwan Lee, MD, PhD,[4,5] Young Hoon Kim, MD,[9] and Jina Ryu, PhD[1]



Recent advances in the field of tissue engineering and regenerative medicine have contributed to the repair of damaged tissues and organs. Renal dysfunctions such as chronic kidney disease (CKD) are considered intractable owing to its cellular heterogeneity. In addition, the absence of definitive treatment options other than dialysis or kidney transplantation in advanced CKD. In this study, we investigated therapeutic effects of a three-dimensional (3D) bio-printed omentum patch as treatment source. Because omentum contains a lot of biological sources for immune regulation and tissue regeneration, it has been used in clinic for >100 years. By using autologous tissue as a bio-ink, the patch could minimize the immune response. The mechanically micronized omentum without any additives became small enough to print, but the original components could be preserved. Then, the 3D printed omentum patch was transplanted under renal subcapsular layer in unilateral ureteral obstruction (UUO) rat model. After 14 days of patch transplantation, the kidneys were analyzed through bulk RNA sequencing and histopathological staining. From the results, decreased tubular injury was observed in the omentum patch group. In addition, the omentum patch significantly altered biological process of gene ontology such as fibrosis-related gene and growth factors. RNA sequencing confirmed the antifibrotic effect by inhibiting fibrosis-inducing mechanisms within PI3K-AKT and JAK-STAT pathways. In conclusion, the omentum patch showed the effect of antitubular injury and antifibrosis on UUO kidneys. In particular, the omentum patch is expected to protect the organ from further degeneration and loss of function by inhibiting the progression of fibrosis. The omentum patch can be a novel therapeutic option for renal dysfunction.

**Keywords:** 3D bio-printer, autologous omentum patch, chronic kidney disease, interstitial fibrosis, UUO model

[1]R&D Center, ROKIT Healthcare, Inc., Seoul, Republic of Korea.
[2]Department of Biomicrosystem Technology, Korea University, Seoul, Republic of Korea.
[3]R&D Center, ROKIT Genomics, Inc., Seoul, Republic of Korea.
[4]Department of Internal Medicine, Seoul National University Boramae Medical Center, Seoul, Republic of Korea.
[5]Department of Internal Medicine, and [6]Translational Medicine Major, Seoul National University College of Medicine, Seoul, Republic of Korea.
[7]Department of Pathology, Seoul National University Boramae Medical Center, Seoul, Republic of Korea.
[8]Department of Pathology, Seoul National University College of Medicine, Seoul, Republic of Korea.
[9]Department of Surgery, Asan Medical Center, University of Ulsan Collage of Medicine, Seoul, Republic of Korea.

### Impact Statement

Many studies and clinical trials are being conducted to develop new treatments for kidney disease. However, there are no newly developed renal replacement therapies. In this study, we developed a new treatment that can ameliorate renal interstitial fibrosis using three-dimensional (3D) bio-printed autologous omentum patch. The 3D printer enables precise patch printing, and the bio-ink made of autologous tissue minimizes the immune response after transplantation. The whole kidneys were analyzed by RNA sequencing and histopathological staining 14 days after transplantation. From the results, the omentum patch had the effect of relieving tubular injury in the injured state. Also, the omentum patch significantly altered biological process of gene ontology. In particular, genes related to fibrosis were observed to be downregulated by the omentum patch. RNA sequencing confirmed that the antifibrotic effect was owing to inducing mechanisms of PI3K-AKT and JAK-STAT pathways. The findings reported in this study represent a significant advancement in the application of 3D bio-printer to damaged organ treatments, especially fibrosis-related diseases.



## Introduction

Chronic kidney disease (CKD) is defined as a progressive loss in renal function. It affects 8–10% of adults worldwide. Millions of people die prematurely each year from complications associated with CKD.[1,2] The US Centers for Disease Control and Prevention (CDC) predicts that 47% of people over the age of 30 will develop CKD during their lifetime.[3] In the 11% of people with stage 3 CKD, lack of proper treatment often drives CKD progression to end-stage renal disease (ESRD), which requires dialysis or a kidney transplant. CKD is also one of the strongest risk factors for cardiovascular complications.[4,5] The cost of treating CKD ($49 billion) is more than double the cost of ESRD ($23 billion).[6] The occurrence of CKD and the progressive renal fibrosis are difficult to treat because of complex signaling pathways and the chronic disease duration.

Therefore, it is important to inhibit the progression for disease via appropriate regulation and mitigation of disease-related stimuli. No definitive treatments are available to abrogate the severely altered histopathological lesions, especially in progressive CKD.[1] To suppress multiple signaling pathways in CKD, several strategies have been attempted including TGF-β inhibitor,[7–9] BMP-7,[10–12] galectin-3 inhibitor,[13–16] and chemokine CCL2.[17–19] However, the effect of treatment was limited owing to poor suppression of fibrosis and adverse effects.[20–22] Therefore, novel treatment options are needed to regulate renal fibrosis and CKD progression.

Omentum has been reported to contain abundant biological sources for immune regulation and tissue regeneration, including anti-inflammatory and antibacterial cytokines.[23,24] It is also large peritoneal fold that hangs from the stomach and wraps around the abdominal organs. Immune cell clusters called ''milky spots'' in omentum play a protective role by adhering to areas of inflammation, and absorbing contaminants for the local immune response. The milky spots of the omentum are clustered between adipocytes and mesothelial cells with leukocytes, mesothelial cells, B cells, macrophages, dendritic cells, T cells, and ILC2.[25] The physiological role of the omentum is not entirely clear, but it has been widely used in surgery for >100 years such as regenerative and reconstructive surgeries.[26]

Several attempts to wrap omentum in the injured area have demonstrated its safety and effectiveness. For example, after lymphorenal disconnection for chyluria, omental wrapping around the renal pedicle increased blood supply and minimized morbidity and recurrence.[27] In gastrointestinal surgery, the omentum surrounding the anastomosis prevented leakage.[28] In gastric perforation, the omental patch promoted wound healing through the combined effects of angiogenesis, granulation, scaffolding, and fibrosis to regenerate.[29]

Three-dimensional (3D) bio-printing is considered as one of the important tools for the scaffolds fabrication to repair or replace damaged tissues or organs. With the principle of layer-by-layer lamination, it is possible to quickly print in a desired shape using autologous biomaterials as bio-ink including extracellular matrix (ECM) and stromal cells with uniform density and porous structure. In particular, use of the ECM as bio-ink has been highlighted in tissue engineering field because of the cellular microenvironment and form of 3D network.[30]

In this study, we evaluated the antifibrotic effects of omentum patch to resolve renal fibrosis induced by unilateral ureter obstruction (UUO) in rat models. To investigate such effects, we fabricated omentum as a bio-ink. Omentum bio-ink was transplanted to subcapsular space of the kidney in an animal model of CKD after 3D bio-printing. Although we evaluated this new approach using 3D bio-printed autologous omentum patch, which can be potentially used to treat CKD as an alternative to pharmacologic therapies associated with side effects.

## Materials and Methods

### *Animals and experimental design*

All animal procedures were conducted according to the Institute of laboratory animal research guide for the care and use of laboratory animals and approved by the Institutional Animal Care and Use Committee (IACUC) of Helixmith Co., Ltd. (VIC-21-10-004; Seoul, Korea). A total of 12 male Sprague-Dawley (SD) rats (average weight, $220 \pm 20$ g) were purchased from Raonbio, Inc. (Yongin, Korea). The rats underwent UUO and were divided into four groups: sham operation with fibrin patch ($n = 3$), sham operation with omental patch ($n = 3$), UUO with fibrin patch ($n = 3$), and UUO with omental patch ($n = 3$). To create a UUO model, the left flank was incised by $\sim 2$ cm, and the left ureter was ligated. A position 0.5 to 1 cm distal to kidney was ligated with a 4.0 suture. Three days after the UUO model development, the autologous omentum was extracted and printed using 3D bio-printer. Then the patch was transplanted in the renal subcapsular layer. All experimental animals were killed 2 weeks after patch transplantation. Rats were anesthetized in a sealed chamber using 5% enflurane in oxygen and maintained by face mask of 2% enflurane.

### Omentum processing and 3D bio-printing

The printing patches were performed by 3D bio-printer (Dr. INVIVO, ROKIT Healthcare, Inc., Seoul, Korea). For bio-ink preparation, autologous omentum was extracted from individual animals and processed using medical grade Dr. INVIVO AI Regen Kit (#ARK-001; ROKIT Healthcare, Inc., Seoul, Korea). All processes were performed while maintaining a sterile state in the operating room. In addition, all surgical devices were sterilized including a 3D printer. We used fibrin glue (Beriplast P, CSL Behring GmbH, Marburg, Germany) for thickening. The optimal ratio of omentum patch components was tested. The bio-ink concentration for the patch is indicated hereunder.

Bio-ink 1: mixture of micronized omentum and 90 mg/mL of fibrinogen
Bio-ink 2: 500 IU/mL of thrombin

We optimized the ratio between omentum and fibrin glue. From different ratios, omentum:fibrinogen:thrombin = 2:4:4 (20% of omentum), 6:2:2 (60% of omentum), and 8:1:1 (80% of omentum), 60% of omentum was selected to be a bio-ink. For the omentum patch printing, we used AI Regen,[31] an AI application that uses computer vision and machine learning technology to automatically generate 3D bio-printable patches. The omentum patch was printed layer-by-layer with bio-inks 1 and 2. The patch was transplanted into renal subcapsular space. As a control, the fibrin patch group was printed by diluting 90 mg/mL fibrinogen, 500 IU/mL thrombin, and saline to 60% volume to match the same concentration as the omentum patch.

### Histopathological analysis

To analyze renal histology and immunohistochemistry, kidneys were embedded in paraffin and sectioned to 4 μm thick specimens. The sectioned tissue was deparaffinized and rehydrated. For Masson's Trichrome (MT) staining, the sectioned tissues were treated with Weigert's iron hematoxylin solution for 10 min to stain the nuclei. Collagen, cytoplasm, and muscle fibers were stained with reducing Biebrich scarlet acid fuchsin solution. Tissues were reacted with phosphomolybdic-phosphotungstic acid solution and stained with aniline blue for 10 min without washing. The nonspecific stained area was removed with 1% acetic acid. For sirius red (SR) staining, slice was stained with picro SR for 60 min at room temperature after incubation with hematoxylin for 10 min.

The tissue slides were placed in distilled water, dehydrated, and mounted. As given in Supplementary Table S1, semiquantitative analysis was performed on whole kidney slides in each group. Depending on the degree of assign, the severity of the change was represented in scores as None (−), Mild (+), Moderate (++), and Severe (+++).[32] Tubular injury score was assessed by tubular dilatation through 5 random fields. Interstitial fibrosis score was randomly evaluated as percentage of MT and SR stained area in 10 fields (each 3 animals) of renal cortical region at 100× magnification using ImageJ software (V1.8; NIH, Bethesda, MD). Fibrosis was examined by a pathologist.

### 4,6-diamidino-2-phenylindole Staining

The extracted omentum was stained with 4,6-diamidino-2-phenylindole (DAPI; Sigma-Aldrich, St. Louis, MO) following micronization method as described previously. Native and micronized omentum was fixed with 4% paraformaldehyde (PFA) and stained with 2 mg/mL DAPI. The stained tissue was imaged with a fluorescence microscope (Eclipse Ts2-FL; Nikon, Tokyo, Japan) after whole mounting.

### RNA isolation, library preparation, and sequencing

After isolation of total RNA from rat kidney sample of all groups, DNA contamination was removed using DNase. To construct cDNA libraries with the TruSeq Stranded mRNA LT Sample Prep Kit (Illumina, San Diego, CA), total RNA was used. The protocol consisted of polyA-selected RNA extraction, RNA fragmentation, random hexamer primed reverse transcription, and 100 nt paired-end sequencing by Illumina NovaSeq 6000 (Illumina, Inc.). The libraries were quantified using qPCR according to the qPCR quantification protocol guide and qualified using an Agilent 2100 Bioanalyzer (Agilent Technologies, Inc., Palo Alto, CA).

### Bioinformatics analysis

Raw reads from the sequencer were preprocessed to remove low-quality and adapter sequence before analysis and processed reads were aligned to the *Rattus norvegicus* using HISAT v2.1.0.[33,34] The reference genome sequence and annotation data were downloaded from the NCBI. Then, the transcript assembly of known transcripts was processed by featureCounts v1.6.0.[35] Based on that result, expression abundance of transcript and gene was calculated as read count or fragments per kilobase of exon per million fragments mapped (FPKM) per sample. The expression profiles were used to do additional analysis such as differentially expressed gene (DEG). It was analyzed by substituting the group average FPKM value, and an absolute fold change (FC) cutoff value of 0.585 (≥1.5 FC) in $\log_2$ scale was utilized to assess dysregulated genes in each group.

In groups with different conditions, DEGs or transcripts can be filtered through statistical hypothesis testing. For differential expressed genes, gene ontology (GO) and Kyoto Encyclopedia of Genes and Genomes (KEGG) were performed with clusterProfiler v 3.18.1 in R v 4.0.3,[36] which supports statistical analysis and visualization of functional profiles for genes and gene clusters. Heatmap package was used to construct heatmap.

### Statistical analysis

Data were statistically analyzed using mean (±standard error of the mean). Difference between repeated measurements of each group was statistically analyzed using analysis of variance or Student's *t*-test, and $***p < 0.001$, $**p < 0.005$, and $*p < 0.05$ were considered statistically significant values. All statistical analyses were performed by Prism 8 (GraphPad, San Diego, CA).

## Results

### 3D Bio-printing of omentum patch and its transplantation

For the 3D bio-printed omentum patch, autologous omentum of rats was extracted and micronized. Omentum has been used in clinic because of its abundant biological

sources.[24] The reticulum-like morphology of blood vessels and fat structures was observed in the rat omentum (Fig. 1A). In a previous study, we confirmed that omentum tissue had become smaller through micronization, enabling printing. In addition, mechanical micronization allowed maintenance of tissue components such as ECM and cells (Fig. 1B). Because the milky spot (yellow arrow in the hematoxylin and eosin image), the dense cell area, is in omentum, there were concerns that the effect of omentum may be uneven if the omentum is used as it is. Cells were distributed unevenly in native omentum, but uniformly distributed cells were observed in the micronized omentum (Fig. 1C).

We developed an omentum and fibrin glue mixture at different ratios of omentum [omentum:fibrinogen:thrombin = 2:4:4 (20% of omentum), 6:2:2 (60% of omentum), and 8:1:1 (80% of omentum)] and discharged it with a syringe (Fig. 1D). When the content of micronized omentum was >80% by volume, it was difficult to maintain a solid shape for application to the damaged kidney. On the contrary, when the content of the micronized omentum was <20% by volume, although it was easy to maintain a patch-like solid shape, the biodegradability was low owing to the high content of fibrin glue. Therefore, we decided to use 60% micronized omentum, which was suitable for printing and had a good biodegradability.

We implanted the 3D printed patch into the subcapsular space of the kidney (Fig. 1E). In this process, we used AI Regen Kit and an AI application that uses computer vision and machine learning technology, to automatically generate 3D printed therapeutic patch.[31] The kidney was photographed, and the patch file was created by hand drawing. After sending the file to Dr. INVIVO, the omentum therapeutic patch was printed and transplanted.

### *Reduced tubular injury in UUO rat model by the omentum patch*

A rat UUO model of CKD was created by ligation of ureter. Significant renal hemodynamic and metabolic changes are induced owing to ureteral obstruction.[37] Severe tubular dilation, interstitial expansion, hydronephrosis, and interstitial fibrosis were observed in the UUO group with fibrin patches compared with the UUO group with omentum patches (Supplementary Table S1). Although it is difficult to

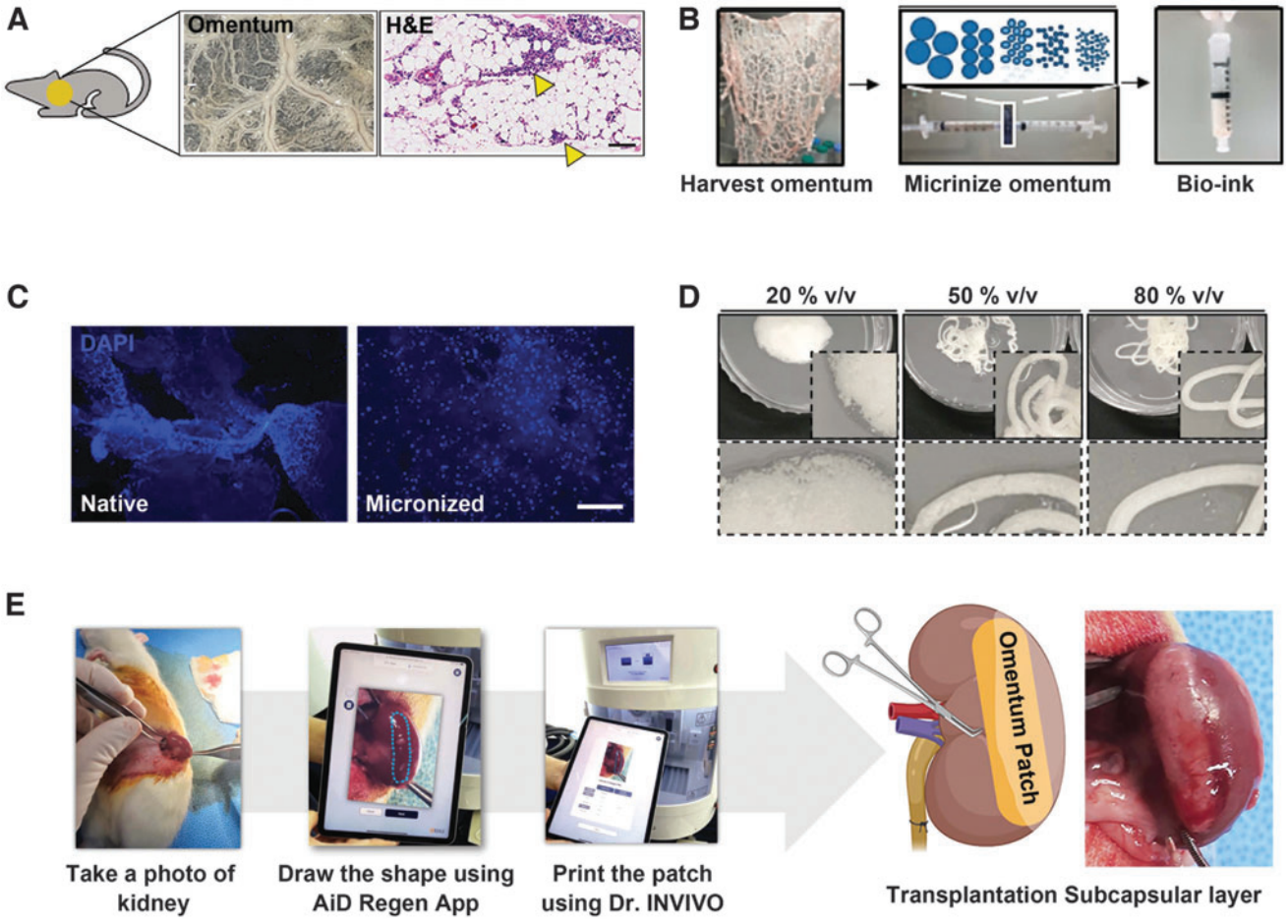


**FIG. 1.** The process of the patch preparing and transplantation. **(A)** Morphological and histological images (H&E) of rat omentum. Milky spot (*yellow arrow*). **(B)** The mechanical process of omentum by micronization. The pore size of 0.2–4.0 mm of mesh filters were used. **(C)** Nuclei fluorescence images of native omentum (*left*) and micronized omentum (*right*) using DAPI staining (scale bar = 100 μm). **(D)** Optimization of the ratio between omentum and fibrin glue. **(E)** AiD Regen was used for the automatic patch printing. The printed omentum patch (30 × 7 × 0.8 mm) was implanted in the subcapsular layer. DAPI, 4,6-diamidino-2-phenylindole; H&E, hematoxylin and eosin. Color images are available online.

confirm the functional effect, the UUO can be easily modeled via ureteral ligation, and has been widely used to represent various CKD histopathological features.[38,39] To validate the surgery, a sham group was included as a control. We observed that kidneys of the UUO group enlarged after the operation by ligated urine pressure (Fig. 2A).

In addition, after 2 weeks of patch applying, the form of patch disappeared. The kidney area (width × length) in the fibrin patch group increased quantitatively up to week 2, whereas the area in the omentum patch group increased until week 1, but there were no significant (ns) changes in week 2 (Fig. 2B). After 2 weeks of UUO, the renal tubule damage-

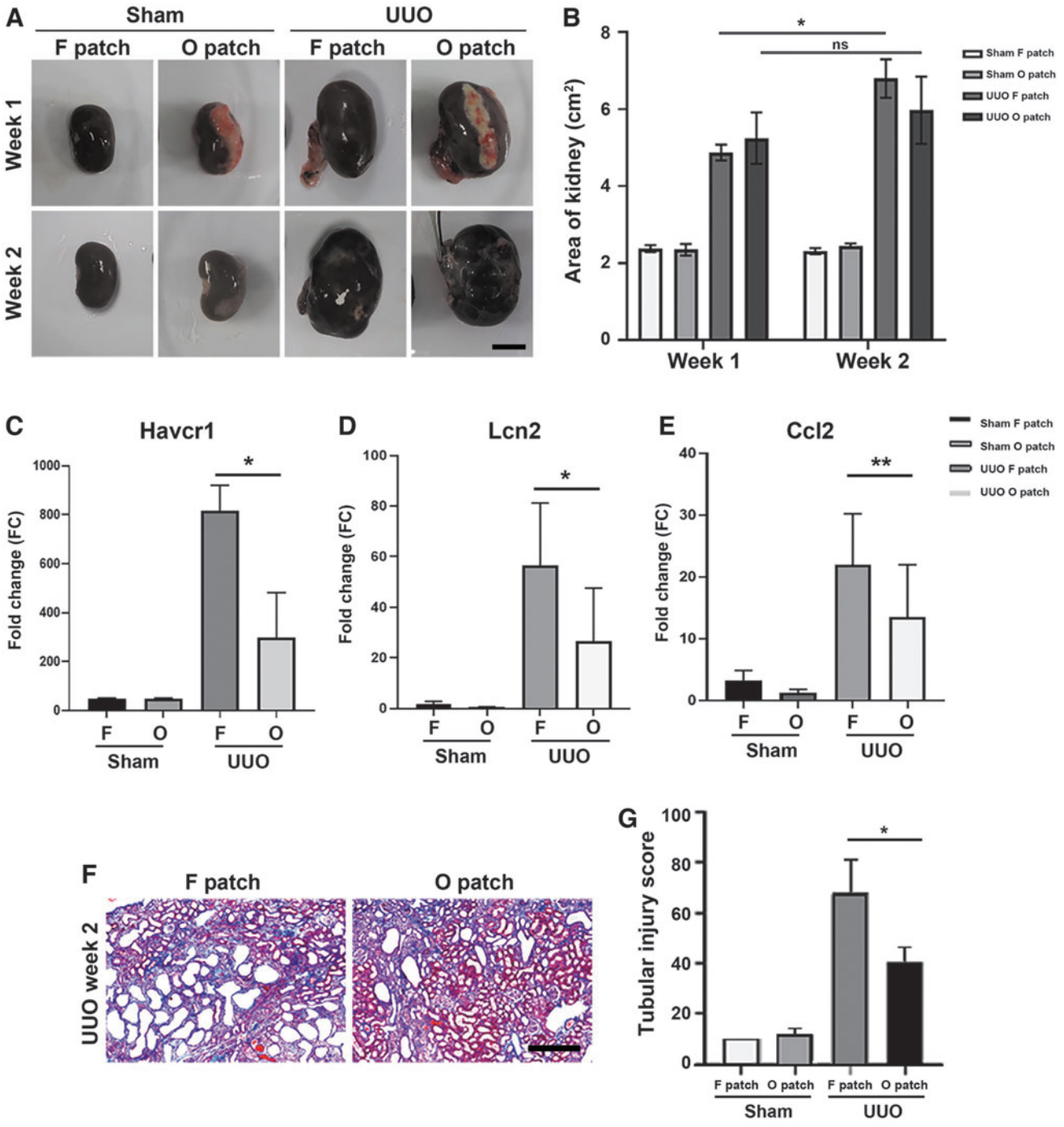


**FIG. 2.** Reduced tubular injury by the omentum patch in the UUO rat model. **(A)** Representative photographs of kidneys in each group. **(B)** The kidney size of rats was quantitatively measured after patch transplantation. The bar graph shows measurements of the kidney area (width × length) with ImageJ ($n = 3$). **(C–E)** At 2 weeks after UUO, gene expression of the renal injury markers was analyzed through RNA sequencing. **(C)** Expression gene level of Havcr1 gene. **(D)** Expression gene level of Lcn2. **(E)** Expression gene level of *Ccl2*. **(F)** Histological staining with MT staining after UUO. Scale bar = 200 μm. **(G)** Quantitative analysis of the degree of tubular dilatation with the tubular injury score. $*p < 0.05$, $**p < 0.005$ ($n = 3$). F patch, fibrin patch; MT, Masson's Trichrome; ns, not significant; O patch, omentum patch; UUO, unilateral ureteral obstruction. Color images are available online.

related genes such as *Havcr1* (encoding KIM-1), *Lcn2* (encoding NGAL), and *Ccl2* (chemokine) were significantly increased in the fibrin patch group, but the omentum patch group had lower gene expressions (Fig. 2C–E). As given in Figure 2F, histopathological analysis (MT staining) demonstrated that UUO-induced tubular injury was histopathologically shown to be tubular dilatation. In the fibrin patch group, tubular dilatation significantly expanded in the renal cortex and medulla.

On the contrary, less tubular dilatation was observed in the omentum patch group. Tubular injury was scored using individual five random fields in each kidney sample[40] (Fig. 2G). In the sham groups, there were no significant differences between the fibrin patch and the omentum patch. However, in the UUO groups, tubular injury score was 0.59 times lower in the omentum patch group than in the fibrin patch group. The omentum patch decreased tubular injury in the UUO model, but there were no changes in the sham groups. Therefore, we concluded that the omentum patch had the effect of relieving tubular injury in the injured state.

### *Regulation of biological process by the omentum patch*

To investigate GO enrichments of the omentum patch, the gene expression level of the kidney in each group was analyzed using bulk RNA sequencing. The GO was selected for biological processes by comparing fibrin versus omentum patch groups after UUO. The predominant 10 up- or downregulated pathway was analyzed (Fig. 3). Of interest, many genes related to epithelial cell proliferation or migration were upregulated in the omentum patch group (Fig. 3A). Because the tubular epithelial cells are responsible to constitute the basic functional units of kidney, the proliferation or recruitment of epithelial cells are important to recovery injured kidney.[41] In addition, the genes related to renal tubule development was upregulated in the omentum patch group compared with that in the UUO control group. The reconstruction of renal tubule plays critical roles in kidney tissue regeneration.[42]

On the contrary, there were downregulated genes in the omentum patch group (Fig. 3B). For example, gene expression of organic anion transport was downregulated. Organic anion transporter expressed in renal proximal tubules cells is known as a role for elimination of metabolic waste or toxins.[43] Moreover, mononuclear cell differentiation and response to toxic substance for anti-inflammatory response were downregulated in the omentum patch group. These genes changes occurred only in the UUO groups, and did not appear in the shame groups. It indicates that this is not a gene expression of omentum cells, but rather a change in kidney cells owing to the active component of omentum. Therefore, we concluded that the omentum patch regulates biological processes to recover damaged kidneys.

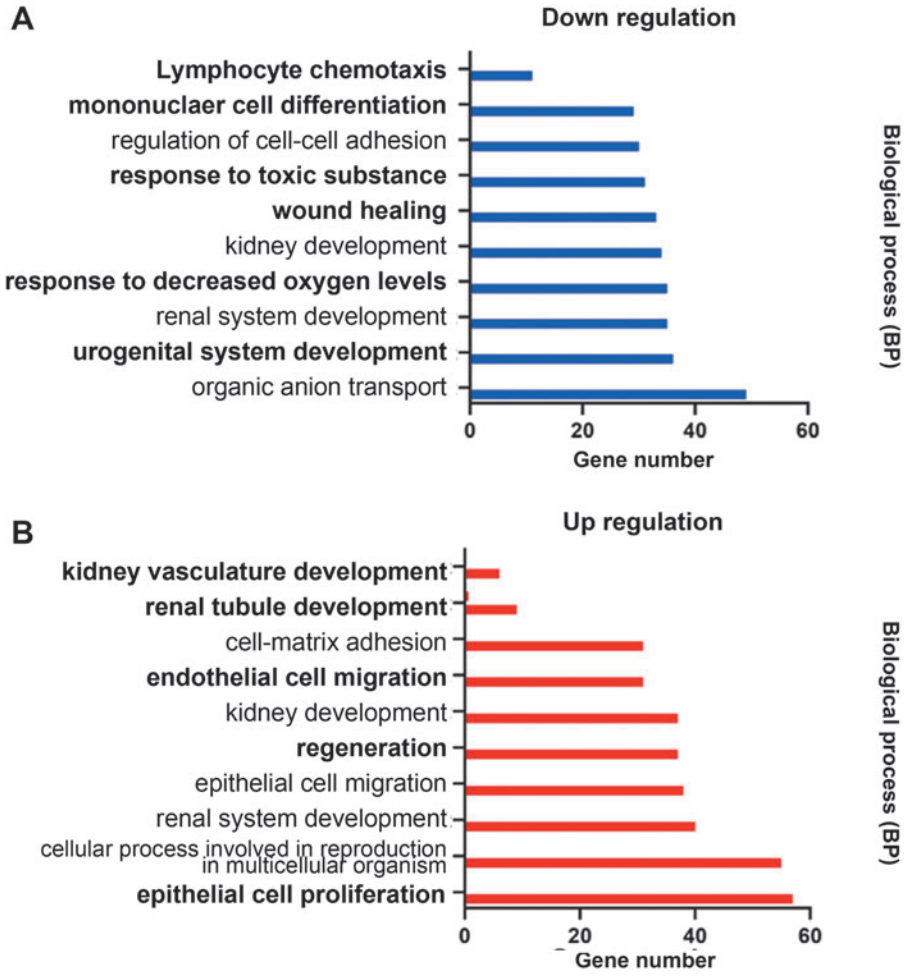


**FIG. 3.** GO analysis of biological processes in omentum patch group after UUO. Top 10 of the predominant upregulated (*red*) **(A)** and downregulated (*blue*) genes **(B)** indicates biological process of GO enrichment between UUO groups (fibrin patch vs. omentum patch) ($n = 3$). GO, gene ontology. Color images are available online.

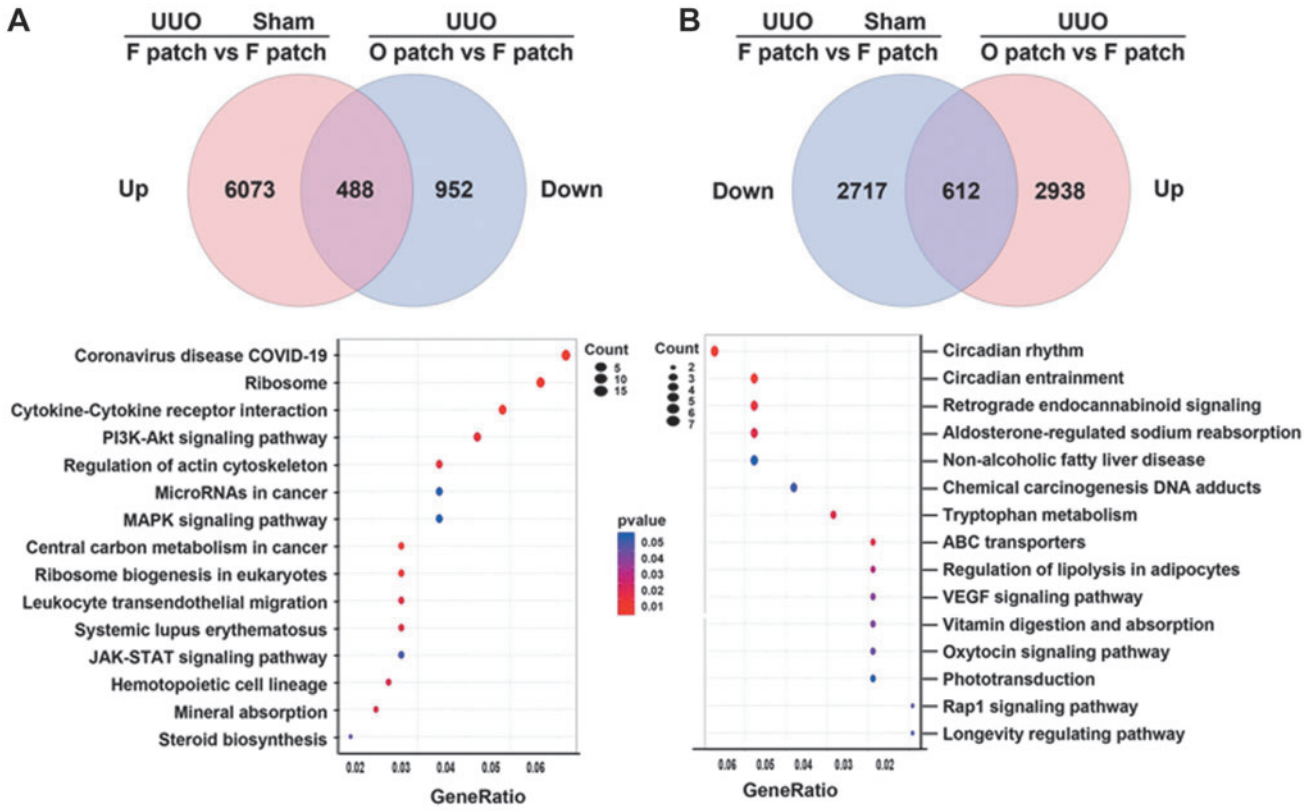


**FIG. 4.** Pathway analysis of contraregulated DEGs using KEGG. **(A)** In the Venn diagram, 488 contraregulations genes were expressed, and were compared between groups (up in UUO + F patch/Sham+F patch vs. down in UUO + O patch/UUO+F patch); top 15 enriched KEGG pathways were observed. **(B)** The top 15 pathways were conversely related to 612 contraregulated genes (down- in UUO + F patch/Sham+F patch vs. up- in UUO + O patch/UUO+F patch). Counts of matched genes represent spot sizes, and the color gradient represents the *p*-value in the analysis pathway ($n = 3$). DEGs, differentially expressed genes; KEGG, Kyoto Encyclopedia of Genes and Genomes. Color images are available online.

### *KEGG pathway in the omentum patch group*

Transcripts were visualized by pathway analysis through KEGG. We performed pathway enrichment analysis on the contraregulated DEGs identified from ''UUO or sham with fibrin patch'' versus ''UUO with fibrin or omentum patch'' (Fig. 4). In the differentially expressed genes analysis of UUO fibrin patch versus sham fibrin patch, it was observed that ureteral obstruction induced 6561 gene upregulation (Fig. 4A). On the contrary, 1440 genes were downregulated by applying the omentum patch.

In conclusion, 488 of the genes increased by UUO were lowered by the omentum patch. Top 15 enriched KEGG pathways were listed. Counts of matched genes represent spot sizes, and the color gradient represents the *p*-value in the analysis pathway ($n = 3$). From the results, fibrosis signaling including PI3K-AKT, JAK-STAT, and MAPK, which were raised by UUO, were observed to reduce after applying the omentum patch. In Figure 4B, 612 of the 3329 genes decreased by UUO were upregulated by the omentum patch. All data suggest that the omentum patch helps kidney recovery by regulating the valence of genes that are abnormally up- and downregulated by UUO.

### *Effects of renal interstitial fibrosis induced by UUO*

Because a decrease in fibrosis signals was observed, we analyzed for the anti-interstitial sclerosis effect of the omentum patch on the kidneys by bulk RNA sequencing. To evaluate the interstitial sclerosis, we selected fibrosis-related

**FIG. 5.** Effect of omental patch on renal interstitial fibrosis induced by UUO in rats. **(A)** The heat map shows renal fibrosis-related gene sets in the omentum patch group (O patch) compared with the fibrin patch group (F patch) after UUO using RNA sequencing. Heatmap is a numerical measurement method through z-score for a value's relationship ($n = 3$). Student's *t*-test. **(B)** Relative quantitative analysis of renal fibrosis marker gene expression compared with the sham fibrin patch group (control) at 2 weeks after UUO. **(C)** Histopathological analysis of renal interstitial fibrosis. MT (fibrosis; *blue*) and SR (fibrosis; *red*) staining for assessing collagen deposition in the fibrotic area at 2 weeks after patch transplantation post-UUO. Applied group of fibrin patch (1st, 3rd column) as control, transplantation of omental patch (2nd, 4th column). Scale bar = 200 μm. **(D)** Quantitative analysis of MT expression area (*blue*). **(E)** Relative analysis of SR-expression area (*red*) by 10 random fields in cortex (magnification 200×) compared with 4 groups. $*p < 0.05$, $**p < 0.005$, $***p < 0.001$ ($n = 3$). SR, sirius red. Color images are available online.

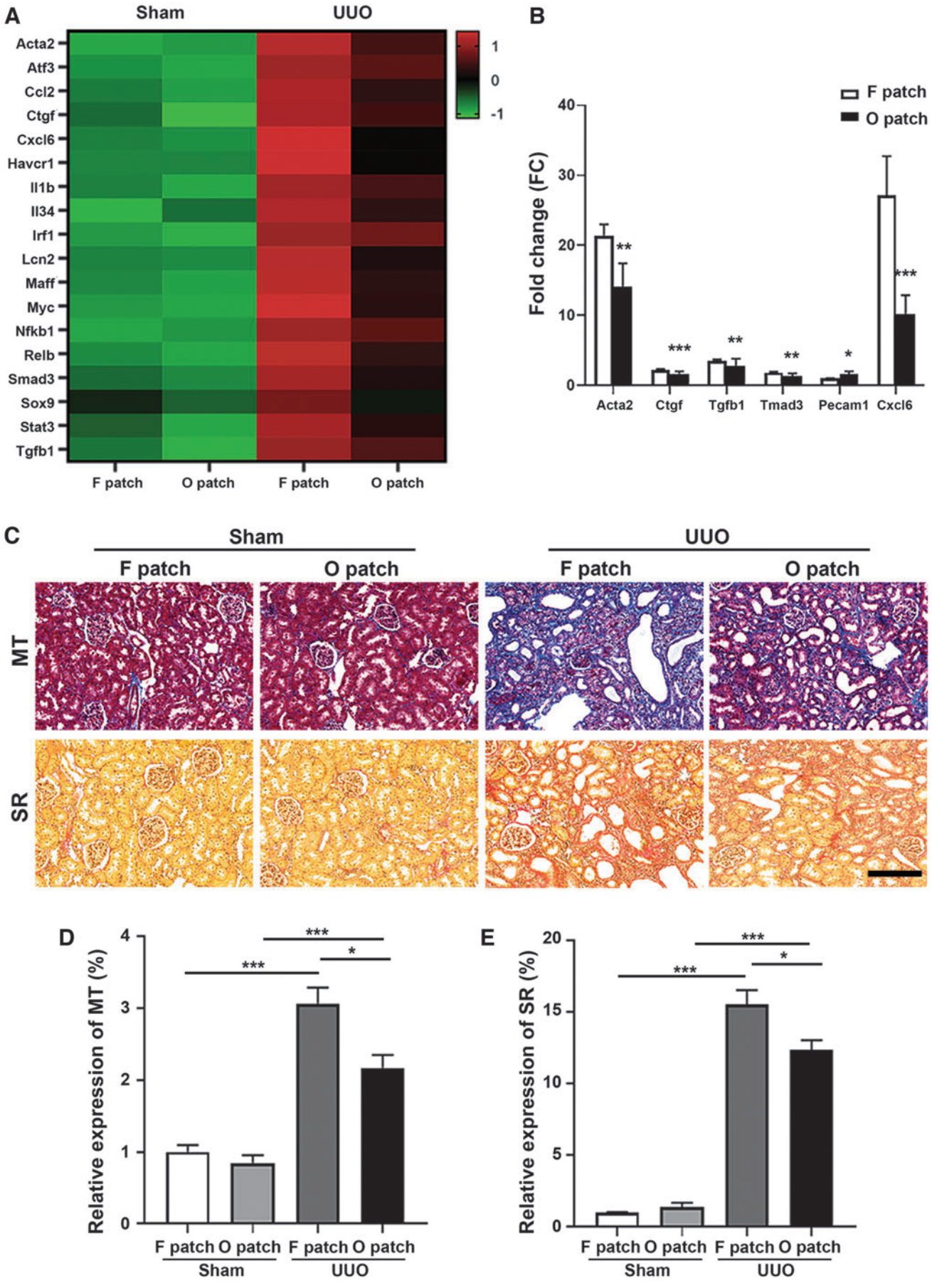

genes including *Acta2, Ctgf, Smad3, Cxcl6, Ccl2, Havcr1, Lcn2, Sox9* (SRY-box 9), and *Maff*,[44] as well as profibrotic transcription factors including I*rf1, Nf-kb1, Stat3,* and *Tgfb1*[45] as gene sets. From the heat map, we observed that profibrotic or fibrotic-related genes were upregulated in the fibrin patch group, but not in the omentum patch group (Fig. 5A). From the result of quantitative analysis, the expression of fibrosis markers such as *Acta2, Ctgf, Tgfb1, Smad3,* and *Cxcl6* was significantly lower in the omentum patch group compared with that in the fibrin patch group (Fig. 5B).

However, the endothelial cell marker, *Pecam1*, was 1.6 times higher in the omentum patch group compared with that in the fibrin patch group. MT staining (fibrosis; blue) and SR staining (fibrosis; red) were performed to evaluate interstitial fibrosis (Fig. 5C). Fibrosis accumulation was histopathologically observed in kidney cortex after 2 weeks of UUO. Renal fibrosis on the transverse sectioned kidney over all area was scored by a histologist. As given in Figure 5D and E, the MT and SR stained areas increased 3.06-folds in the fibrin patch group and 2.1-folds in the omentum patch group of UUO kidney compared with that in the sham group, respectively. From the results, fibrosis scores were higher in the fibrin patch group compared with those in the omentum patch group. Together, these findings suggest that the omentum patch played a role in lowering renal fibrosis in the rat UUO model.

## Discussion

In this study, we demonstrated that the micronized omentum was used as a bio-ink for kidney treatment. Through physical micronization, the omentum tissue could be used as a bio-ink by reducing the size and removing fibers. In addition, because there was no chemical treatment for ink preparation, cellular components and micro size ECM remained in the ink without affecting cell viability.[46] It is known that micronization of adipose tissue can lead to mechanical disaggregation, and extraction of components including cells and growth factors that promote cell viability, proliferation, and differentiation of the natural matrix after transplantation.[47–49] Therefore, we utilized micronization for processing omentum, and the micronized omentum was applied to 3D printing with adequate viscosity (Fig. 1).

After applying the ometum patch to kidneys, we analyzed the whole transcriptome. Among 38,000 genes, the differences in gene expression of each group were observed. In addition, the biological functions and pathways were identified by whole transcriptome analysis combined with bioinformatics analysis. We observed that genes related to proliferation of fibroblast such as *Ccl2, Myc, Relb,* and *Sox9* were upregulated in UUO groups compared with that in the sham groups. In addition, the expression of CKD-related genes including *Acta2* (a-SMA), *Ctgf, Tgfb1, Smad3,* and *Cxcl6* were increased after ureteral obstruction. Shunsakju et al showed increased expression of *Havcr1* and *Lcn2* in several forms of CKD, and their expression levels were correlated with tubular interstitial fibrosis and tubular cell damage.[44] Of interest, despite the obstruction, the FPKM values of fibrosis-related genes were greatly reduced in the omental patch group.

It is known that a rarefaction of peritubular capillaries in kidney occurred in fibrosis.[50] In Figure 5B, we observed 1.6 times higher expression of endothelial cell marker, *Pecam1*, in the omentum patch group compared with that in the fibrin patch group. This indicates that the omentum patch could inhibit the rarefaction in peritubular capillaries. To confirm the effect of omentum on capillary rarefaction, imaging analysis such as IHC or IF is required for further study. GO results showed that while many genes were expressed in the omentum patch group with UUO, the omentum patch applied to shame model did not induce gene expression. Therefore, we assume that the valid ingredient of omentum is activated by signals from injured kidneys, and that the ingredient as a paracrine factor regulates genes for kidney recovery, such as inhibiting fibrosis-related genes.

Because tubular injury is caused by tubular dilatation, interstitial dilatation, and hydronephrosis in the injured kidney after UUO, we analyzed signaling focusing on renal injury and fibrosis. We observed some upregulated fibrosis signaling in UUO with the fibrin patch group including PI3K-AKT,[51] JAK-STAT,[52] and MAPK.[53] However, in the omentum patch group, the fibrosis signaling was not activated much even after UUO. Then, we investigated that the recovery effect of the omentum patch after renal injury was related to the PPAR signaling pathway through KEGG analysis of the transcriptome. PPAR gamma is known to be expressed in the collecting duct of the kidney, podocytes, mesangial cells, and vascular endothelial cells.[54,55] Furthermore, it is known to play an important role in kidney function, especially in antifibrotics.[56] In the results, we observed upregulation of PPAR signaling-related genes including *Me1, Cpt1b, Rxrg, Acox2,* and *Pck1* in the omentum patch group compared with the fibrin patch group after UUO.

Finally, we observed that genes related to retinol metabolism, such as *Cyp1a1, Aldh1a7, Aox1, Adh7,* and *Ugt1a9* were upregulated in the omentum patch of UUO group than in the fibrin patch of UUO group. Retinoids have been shown to exert both protective and preventive effects in various kidney disease animal models through improving podocyte injury, including differentiation of kidney progenitor cells, and attenuating inflammation and apoptosis of the kidney cells.[57] All data suggest that the omentum patch regulated the role in inhibiting renal injury in UUO model.

This study has limitations. The number of animals used in each group was not sufficient for a more robust statistical analysis of the data collected. Nevertheless, we suggest the omentum patch efficiency in the UUO model with demonstrated gene set and histopathology analysis. The kidney is composed of a complex vascular mass and a dense structure; it is difficult to deliver therapeutic substances using traditional delivery methods. A possible mechanism of recovery is that stem cells from the kidney capsule layer are recruited as paracrine effects of the omentum. There is a stem cell niche in the renal capsule layer, and the omentum patch can play a role in boosting cells through paracrine effects.[58]

In this study, it can be manufactured within 30 min in various shapes and thicknesses and can be freely customized and modeled according to the characteristics of tissues and organs. Furthermore, the type of patch manufactured in this study enabled for controlled release of the omentum component. When transplanting cells for regeneration to damaged tissue, encapsulation is required to maintain cell viability and function[59] and therefore, the transplantable patches that use micronized omentum are a new approach for therapeutic omentum.

In conclusion, we demonstrated that omentum patch transplantation for damaged kidneys can ameliorate renal fibrosis in the UUO model. The transplanted omentum patch can help cellular repair and antifibrotic effects, thereby protecting the kidney. In addition, it can prevent ESRD progression and block fibrosis by reducing fibrotic factors. As a novel approach to attenuating fibrosis in patients with CKD, the autologous 3D bio-printed patch technology has shown therapeutic potential in tissue repair and regenerative medicine. Further studies are required to demonstrate a more minimally invasive method and a CKD model to confirm renal function. These findings suggest the potential use of autologous 3D omentum patches for renal fibrosis and other organs.

### Authors' Contributions

H.J., B.Y.C.: study design, executing experiments, writing the article; G.J.: collecting and analyzing data; J.P.L., J.L.: study design, analyzing data; A.C., B.K.: executing experiments; J.H.P., Y.H.K.: analyzing data; J.R.: study design, writing the article.

### Statement of Ethics

Animal experiments conform to internationally accepted standards and have been approved by the Institutional Animal Care and Utilization Committee of Helixmith, Inc., (Seoul, Korea).

### Disclosure Statement

H.J., B.Y.C., B.K., and J.R. are employees of ROKIT Healthcare, Inc.

### Funding Information

This research was funded by ROKIT Healthcare Inc., located in Seoul, Republic of Korea.

### Supplementary Material

Supplementary Table S1

### References

1. Nahas AME, Bello AK. Chronic kidney disease: The global challenge. Lancet 2005;365(9456):331–340.
2. Bello AK, Alrukhaimi M, Ashuntantang GE et al. Complications of chronic kidney disease: Current state, knowledge gaps, and strategy for action. Kidney Int Suppl (2011) 2017; **7**(2):122–129.
3. Benjamin D. Humphreys. Annual review of physiology mechanisms of renal fibrosis. Annu Rev Physiol 2018;80: 309–326.
4. Schiffrin EL, Lipman ML, Mann JF. Chronic kidney disease: Effects on the cardiovascular system. Circulation 2007;116(1):85–97.
5. Thomas R, Kanso A, Sedor JR. Chronic kidney disease and its complications. Prim Care 2008;35(2):329–344.
6. Rashid I, Katravath P, Tiwari P, et al. Hyperuricemia—A serious complication among patients with chronic kidney disease: A systematic review and meta-analysis. Explor Med 2022;3(3):249–259.
7. López-Hernández FJ, López-Novoa JM. Role of TGF-β in chronic kidney disease: An integration of tubular, glomerular and vascular effects. Cell Tissue Res 2012;347(1):141–154.
8. Xavier S, Vasko R, Matsumoto K, et al. Curtailing endothelial TGF-β signaling is sufficient to reduce endothelial-mesenchymal transition and fibrosis in CKD. J Am Soc Nephrol 2015;26(4):817–829.
9. Meng X-M, Nikolic-Paterson DJ, Lan HY. TGF-β: The master regulator of fibrosis. Nat Rev Nephrol 2016;12(6):325–338.
10. Patel SR, Dressler GR. BMP7 signaling in renal development and disease. Trends Mol Med 2005;11(11):512–518.
11. Zeisberg M, Kalluri R. Reversal of experimental renal fibrosis by BMP7 provides insights into novel therapeutic strategies for chronic kidney disease. Pediatr Nephrol 2008;23(9):1395–1398.
12. Manson SR, Austin PF, Guo Q, et al. BMP-7 signaling and its critical roles in kidney development, the responses to renal injury, and chronic kidney disease. Vitam Horm 2015;99:91–144.
13. O'Seaghdha CM, Hwang S-J, Ho JE, et al. Elevated galectin-3 precedes the development of CKD. J Am Soc Nephrol 2013;24(9):1470–1477.
14. Rebholz CM, Selvin E, Liang M, et al. Plasma galectin-3 levels are associated with the risk of incident chronic kidney disease. Kidney Int 2018;93(1):252–259.
15. Henderson NC, Mackinnon AC, Farnworth SL, et al. Galectin-3 expression and secretion links macrophages to the promotion of renal fibrosis. Am J Pathol 2008;172(2):288–298.
16. Martinez-Martinez E, Ibarrola J, Calvier L, et al. Galectin-3 blockade reduces renal fibrosis in two normotensive experimental models of renal damage. PLoS One 2016;11(11): e0166272.
17. Anders H-J, Vielhauer V, Schlöndorff D. Chemokines and chemokine receptors are involved in the resolution or progression of renal disease. Kidney Int 2003;63(2):401–415.
18. De Lema GP, Maier H, Franz TJ, et al. Chemokine receptor Ccr2 deficiency reduces renal disease and prolongs survival in MRL/lpr lupus-prone mice. J Am Soc Nephrol 2005;16(12): 3592–3601.
19. Kashyap S, Osman M, Ferguson CM, et al. Ccl2 deficiency protects against chronic renal injury in murine renovascular hypertension. Sci Rep 2018;8(1):1–12.
20. Nastase MV, Zeng-Brouwers J, Wygrecka M, et al. Targeting renal fibrosis: Mechanisms and drug delivery systems. Adv Drug Deliv Rev 2018;129:295–307.
21. Lv W, Booz GW, Wang Y, et al. Inflammation and renal fibrosis: Recent developments on key signaling molecules as potential therapeutic targets. Eur J Pharmacol 2018;820:65–76.
22. Tampe D, Zeisberg M. Potential approaches to reverse or repair renal fibrosis. Nat Rev Nephrol 2014;10(4):226–237.
23. Chandra A, Srivastava RK, Kashyap MP, et al. The anti-inflammatory and antibacterial basis of human omental defense: Selective expression of cytokines and antimicrobial peptides. PLoS One 2011;6(5):e20446.
24. Nicola V. Omentum a powerful biological source in regenerative surgery. Regen Ther 2019;11:182–191.
25. Meza-Perez S, Randall TD. Immunological functions of the omentum. Trends Immunol 2017;38(7):526–536.
26. Litbarg NO, Gudehithlu KP, Sethupathi P, et al. Activated omentum becomes rich in factors that promote healing and tissue regeneration. Cell Tissue Res 2007;328(3):487–497.
27. Dalela D, Gupta VP, Goel A, et al. Omental wrap around the renal pedicle: An adjunctive step to minimize morbidity and recurrence after lymphorenal disconnection for chyluria. BJU Int (Papier) 2004;94(4):673–674.
28. Dai JG, Zhang ZY, Min JX, et al. Wrapping of the omental pedicle flap around esophagogastric anastomosis after esophagectomy for esophageal cancer. Surgery 2011;149(3):404–410.

29. Raj BR, Subbu K, Manoharan G. Omental plug closure of large duodenal defects an experimental study. Trop Gastroenterol 1997;18:180–182.
30. Zhu M, Li W, Dong X, et al. In vivo engineered extracellular matrix scaffolds with instructive niches for oriented tissue regeneration. Nat Commun 2019;10:4620.
31. Chae HJ, Lee S, Son H, et al. Generating 3D bio-printable patches using wound segmentation and reconstruction to treat diabetic foot ulcers. Proc IEEE/CVF Conf CVPR 2022;2539–2549.
32. Sener U, Uygur R, Aktas C, et al. Protective effects of thymoquinone against apoptosis and oxidative stress by arsenic in rat kidney. Ren Fail 2016;38(1):117–123.
33. Kim D, Langmead B, Salzberg SL. HISAT: A fast spliced aligner with low memory requirements. Nat Methods 2015;12(4):357–360.
34. Pertea M, Kim D, Pertea GM, et al. Transcript-level expression analysis of RNA-seq experiments with HISAT, StringTie and Ballgown. Nat Protoc 2016;11(9):1650–1667.
35. Anders S, Pyl PT, Huber W. HTSeq-A python framework to work with high-throughput sequencing data. Bioinformatics 2014;31:166–169.
36. Yu G, Wang LG, Han Y, et al. cluster Profiler: An R package for comparing biological themes among gene clusters, OMICS 2012;16(5):284–287.
37. Martínez-Klimova E, Aparicio-Trejo OE, Tapia E, et al. Unilateral ureteral obstruction as a model to investigate fibrosis-attenuating treatments. Biomolecules 2019;9(4):141.
38. Chevalier RL, Forbes MS, Thornhill BA. Ureteral obstruction as a model of renal interstitial fibrosis and obstructive nephropathy. Kidney Int 2009;75(11):1145–1152.
39. Wakui H, Yamaji T, Azushima K, et al. Effects of Rikkunshito treatment on renal fibrosis/inflammation and body weight reduction in a unilateral ureteral obstruction model in mice. Sci Rep 2020;10(1):1782.
40. Quan Y, Park W, Jin J, et al. Sirtuin 3 activation by honokiol decreases unilateral ureteral obstruction-induced renal inflammation and fibrosis via regulation of mitochondrial dynamics and the renal NF-κBTGF-β1/Smad signaling pathway. Int J Mol Sci 2020;8(21):402.
41. Sorokin L, Klein G, Mugrauer G, et al. Development of kidney epithelial cells. (eds) Epithelial Organization and Development. Dordrecht: Springer; 1992; pp. 163–190.
42. Andrianova NV, Buyan MI, Zorova LD, et al. Kidney cells regeneration: Dedifferentiation of tubular epithelium, resident stem cells and possible niches for renal progenitors. Int J Mol Sci 2019;20(24):6326.
43. Wang L, Sweet DH. Renal organic anion transpoter (SLC22 family): Expression, regulation, roles in toxicity, and impact on injury and disease. AAPS J 2013;15(1):53–69.
44. Nakagawa S, Nishihara K, Miyata H, et al. Molecular markers of tubulointerstitial fibrosis and tubular cell damage in patients with chronic kidney disease. PLoS One 2015;10(8):e0136994.
45. Wu H, Lai CF, Chang-Panesso M, et al. Proximal tubule translational profiling during kidney fibrosis reveals proinflammatory and long noncoding RNA expression patterns with sexual dimorphism. JASN 2020;31:23–38.
46. Kesavan R, Sasikumar CS, Narayanamurthy VB, et al. Management of diabetic foot ulcer with MA-ECM using 3D bioprinting technology-An innovative approach. Int J Low Extrem Wounds 2021;12:15347346211045625.
47. Alexander R. Understanding mechanical emulsification (nanofat) versus enzymatic isolation of tissue stromal vascular fraction (tSVF) cells from adipose tissue: Potential uses in biocellular regenerative medicine. J Prolother 2016;8:e947–e960.
48. Bayoussef Z, Dixon JE, Stolnik S, et al. Aggregation promotes cell viability, proliferation, and differentiation in an in vitro model of injection cell therapy. J Tissue Eng Regen Med J Tissue Eng Regen M 2012;6(10):e61–e73.
49. Sesé B, Sanmartín JM, Ortega B, *et al.* Nanofat cell aggregates: A nearly constitutive stromal cell inoculum for regenerative site-specific therapies. Plast Reconstr Surg 2019;144(5):1079.
50. Kramann R, Dirocco DP, Maarouf O, et al. Matrix-producing cells in chronic kidney disease: Origin, regulation, and activation. Curr Pathobiol Rep 2013;1(4):301–311.
51. Liu Y, Su YY, Yang Q, et al. Stem cells in the treatment of renal fibrosis: A review of preclinical and clinical studies of renal fibrosis pathogenesis. Stem Cell Res Ther 2021;12(1):333.
52. Kuratsune M, Masaki T, Hirai T, et al. Signal transducer and activator of transcription 3 involvement in the development of renal interstitial fibrosis after unilateral ureteral obstruction. Nephrology (Carlton) 2007;12(6):565–571.
53. Li Z, Liu X, Wang B, et al. Pirfenidone suppresses MAPK signalling pathway to reverse epithelial-mesenchymal transition and renal fibrosis. Nephrology (Carlton) 2017;22(8):589–597.
54. Yang T, Michele DE, Park J, et al. Expression of peroxisomal proliferator-activated receptors and retinoid X receptors in the kidney. Am J Physiol 1999;277(6):F966–F973.
55. Kiss-Tóth E, Roszer T. PPARgamma in kidney physiology and pathophysiology. PPAR Res 2008;2008:183108.
56. Corrales P, Izquierdo-Lahuerta A, Medina-Gómez G. Maintenance of kidney metabolic homeostasis by PPAR gamma. Int J Mol Sci 2018;19(7):2063.
57. Chen A, Liu Y, Lu Y, et al. Disparate roles of retinoid acid signaling molecules in kidney disease. Am J Physiol Renal Physiol 2021;320(5):F683–F692.
58. Park HC, Kaoru Y, Kuo MC, et al. Renal capsule as a stem cell niche. Am J Physiol Renal Physiol. 2010;298(5): F1254–F1262.
59. Kim H, Bae C, Kook Y-M, et al. Mesenchymal stem cell 3D encapsulation technologies for biomimetic microenvironment in tissue regeneration. Stem cell res ther 2019;10(1):1–14.

Address correspondence to:
*Jina Ryu, PhD*
*R&D Center, ROKIT Healthcare, Inc.*
*9 Digital-ro 10-gil, Geumcheon-gu*
*Seoul 08514*
*Republic of Korea*

*E-mail:* jina.ryu@rokit.co.kr

*Received: September 7, 2022*
*Accepted: October 26, 2022*
*Online Publication Date: December 13, 2022*